Paddling Mode of Forward Flight in Insects

Leif Ristroph,[1] Attila J. Bergou,[2] John Guckenheimer,[3] Z. Jane Wang,[1,4] and Itai Cohen[1]

[1]*Department of Physics, Cornell University, Ithaca, New York 14853, USA*
[2]*Department of Engineering, Brown University, Providence, Rhode Island 02912, USA*
[3]*Department of Mathematics, Cornell University, Ithaca, New York 14853, USA*
[4]*Theoretical and Applied Mechanics, Cornell University, Ithaca, New York 14853, USA*

By analyzing high-speed video of the fruit fly, we discover a swimminglike mode of forward flight characterized by paddling wing motions. We develop a new aerodynamic analysis procedure to show that these insects generate drag-based thrust by slicing their wings forward at low angle of attack and pushing backwards at a higher angle. Reduced-order models and simulations reveal that the law for flight speed is determined by these wing motions but is insensitive to material properties of the fluid. Thus, paddling is as effective in air as in water and represents a common strategy for propulsion through aquatic and aerial environments.

PACS numbers: 47.63.−b, 87.85.gf

Despite their apparent differences, swimming and flying animals share similar force generation strategies [1,2]. The lift-based mechanism uses the fluid force generated perpendicular to the direction of travel of a moving appendage. For example, many hovering insects use lift to balance body weight by flapping their wings back-and-forth in a horizontal plane [3]. Similarly, a broad class of both swimming and flying animals employ lift for forward motion by oscillating their hydro- or air-foil appendages up-and-down [4,5]. For forward flight in insects, previous studies have emphasized this mode in which lift is redirected for thrust by forward tilting of the wing stroke planes [6–10].

On the other hand, the drag-based mechanism is associated with paddling or rowing motions and is largely viewed as an aquatic phenomenon [4,11]. For example, this mode is prevalent among swimmers including ciliated micro-organisms [2], semiaquatic birds and mammals [12], as well as fish that use pectoral fins [13]. However, recent work indicates that drag is important for hovering flight in some insects [14,15]. Is drag also used by flying animals for propulsion?

Here, we examine drag-based thrust generation in the flight of insects. We use high-speed video cameras to capture flight sequences of the fruit fly, *D. melanogaster*, and extract the wing and body kinematics using a custom motion tracking algorithm [16]. We find that forward flight can occur even when the wing stroke planes remain nearly horizontal, as shown in Fig. 1. This indicates that these insects have an additional propulsion mechanism distinct from the lift-based mode of stroke-plane tilting. To investigate thrust production in this new mode, we analyze 140 forward flight movies and select the 16 steady flight sequences in which forward acceleration is less than 0.15 g and the stroke planes are oriented within 5° of horizontal. These sequences include body speeds ranging from 2 to 47 cm/s.

The wing adjustments that generate these large differences in forward speed are most easily discerned by contrasting the kinematics of slow and fast flight. In both cases, each wing sweeps along a globe centered about its root on the body [Fig. 2(a)]. The wing motions are visualized by the stroke diagrams associated with hovering flight [Fig. 2(b)] and fast forward flight [Fig. 2(c)]. Both slow and fast flight are characterized by horizontal stroke planes with the forward and backward sweeps separated by rapid wing flips. These kinematics can also be quantified by the time course of three orientation angles: stroke measured in the horizontal plane, vertical deviation, and pitch. In Figs. 2(d)–2(f), we compare the measured angular data for sequences at flight speeds of 2 cm/s (blue) and 43 cm/s (red). Differences can be seen for the time courses
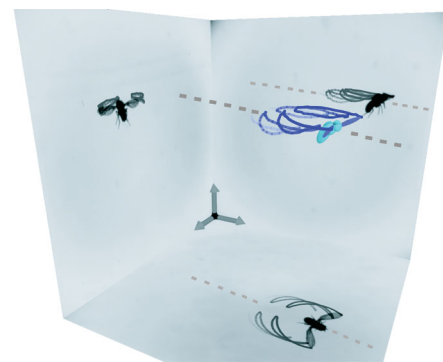

FIG. 1 (color). Reconstruction of forward flight in a fruit fly (body length 2.7 mm). Flight is recorded using three high-speed video cameras, and snapshots from each are displayed on the panels. Body and wing motions are extracted using a tracking algorithm, and these data are displayed on the rendered insect for one frame. The wings beat in horizontal arcs, and wing-tip trajectories for two strokes are shown in dark blue.
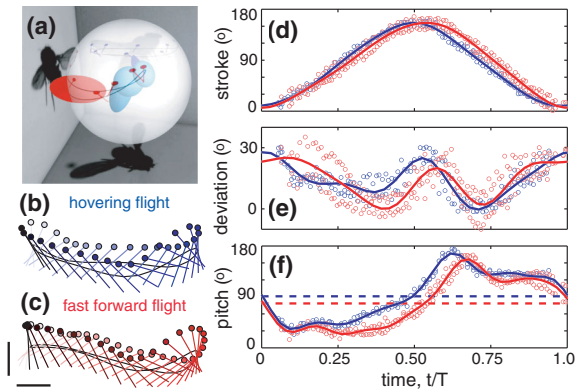
FIG. 2 (color). Comparison of hovering (speed $u = 2$ cm/s) and fast flight ($u = 43$ cm/s). (a) Each wing sweeps along a globe centered about its root on the body [17]. (b and c) Stroke diagrams show the wing as a line with a leading-edge circle (scale bars, 30°). The wings are darker with time and displayed at the frame rate of 8000 Hz. (d–f) Wing angles for hovering (blue, wing-beat period $T = 4.0$ ms) and forward flight (red, $T = 4.8$ ms). Stroke is the angle in the horizontal plane, deviation is the vertical excursion, and pitch is measured between the wing chord and the horizontal. Measurements (circles) are phase-averaged, and right and left wing data are pooled and used to form Fourier fits (solid lines). Mean values of pitch are shown as dashed lines in (f).

of all three angles, suggesting that all three may contribute to thrust generation.

Recent studies of fruit flies have shown that changes in wing pitch play an important role in generating turning maneuvers [17,18]. For forward flight, we also observe changes in pitch for flight at different speeds. In particular, the curve for pitch during fast flight is shifted downward relative to pitch during slow flight [Fig. 2(f)]. This downward shift can be rationalized by considering its effect on aerodynamic forces on the wings. During the forward stroke, the low value of wing pitch indicates the wing is more horizontal and thus slices through the air. During the backward stroke, the low value of pitch indicates the wing is more vertical, pushing off the air with a broad area exposed to the flow. Thus, a decrease in wing pitch generates rowing or paddling motions that propel the insect forward.

To assess how forward flight is generated by these wing motions, we use a computational simulation that determines the body motion from aerodynamic forces on the wings [17]. The simulation solves the Newton-Euler equations for the articulated wings-body system. Each wing is modeled as a plate connected to the body by a three-axis rotational joint, and fluid forces are computed using a blade-element quasisteady aerodynamic model. In these studies, we constrain the simulation to allow body motion in the forward and backward directions. When measured wing motions are played in the simulation, the computed flight velocities are typically within 10 cm/s of the measured values [Fig. 3(a)].
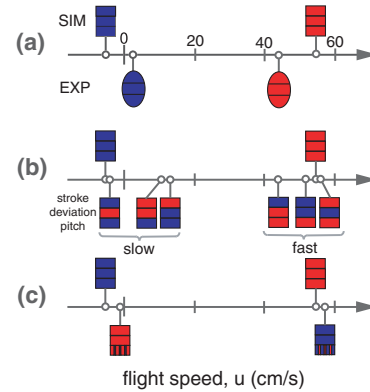

FIG. 3 (color). Dependence of flight speed on wing angles. (a) Comparison of experimentally measured speeds for hovering (blue) and fast flight (red) to those predicted by simulation. (b) Simulations of hovering and fast flight kinematics (top) compared to hybrid kinematics (bottom). For hybrid simulations, wing motions are formed by selecting each angle—stroke, deviation, and pitch—from either the hovering or fast flight set. Slow speeds are associated with pitch from hovering, and high speeds are associated with pitch from fast flight. The remaining spread in speeds is largely due to wing strokes that are faster in their backward sweep [Fig. 2(d)] (c) Simulations of hovering and fast flight (top) compared to those with swapped mean values of pitch (bottom). For example, blue stripes on the red box indicate that the fast flight kinematics have been modified only by shifting the pitch curve upward so as to have hovering's mean value [dashed lines of Fig. 2(f)].

To evaluate the relative importance of the measured changes in wing angles, we develop an aerodynamic analysis procedure that combines measurements and simulations. In Fig. 3(b), we compare the simulations of the complete hovering (blue) and fast flight (red) kinematics to simulations in which the wing kinematic angles are selected from a mix of these two data sets. For example, the color scheme blue-red-blue indicates that the stroke, deviation, and pitch angles are taken from the hovering, fast flight, and hovering sequences, respectively. Simulations of the six possible hybrid kinematics form two distinct groups according to speed. Slow flight speeds are associated with kinematics in which pitch is selected from the hovering sequence, regardless of the sources of the stroke and deviation angles. Conversely, high speeds are associated with pitch selected from fast flight. These results indicate that the changes in wing pitch of Fig. 2(f) are crucial to determining flight speed.

Further, the mean value of pitch, in particular, correlates with flight speed. When the complete hovering kinematics are modified only by shifting the curve for pitch downward so as to have the same mean as that of the fast flight sequence, the simulation yields a speed close to that of the fast flight simulation [Fig. 3(c)]. Conversely, shifting the wing pitch for fast flight upward causes the speed to slow to near zero. Thus, although the wing motions are

complex, much of this flight mode is accounted for by the stroke-averaged value of wing pitch.

These findings inspire a minimal model that includes only changes in average pitch to drive flight at different speeds. Each wing sweeps forward and backwards at constant speed w relative to the body. In hovering, both wings are inclined symmetrically during the forward and backward strokes, with angles of attack between the wing chord and its velocity of $\alpha_F = \alpha_B = \alpha_0 = 45°$ [Fig. 4(a)]. Wing drag, which points opposite to the wing velocity at any instant, cancels over each wing beat, and the insect hovers. Forward flight results from unbalanced drag due to asymmetric attack angles [4,19], $\alpha_F = \alpha_0 - \Delta\alpha$ and $\alpha_B = \alpha_0 + \Delta\alpha$ [Fig. 4(b)]. For these idealized paddling motions, $\Delta\alpha$ corresponds to the downward shift in pitch relative to 90°. As the insect progresses, however, the wing velocities relative to air are modified, causing a resistive drag. Eventually, the drag arising from paddling balances drag due to the forward motion, and the insect achieves a speed u.

To quantify how the attained speed depends on the degree of paddling, we calculate the drag $D = \rho S C_D(\alpha) v^2 / 2$ on a wing of area S and drag coefficient $C_D(\alpha)$ moving at speed v relative to a fluid of density ρ [1,2]. In steady state, the stroke-averaged drag must be zero for the wing pair:

$$D = \tfrac{1}{2}\rho S[-C_D(\alpha_F)(w + u)^2 + C_D(\alpha_B)(w - u)^2] = 0. \quad (1)$$

For small $\Delta\alpha$, we Taylor-expand and linearize the coefficient $C_D(\alpha) = C_D^{max}\sin^2(\alpha)$ [20] about α_0: $C_D(\alpha) \approx C_D(\alpha_0)[1 + 2\Delta\alpha/\tan(\alpha_0)]$. For $\alpha_0 = 45°$, $C_D(\alpha) \approx C_D^{max}(1 + 2\Delta\alpha)/2$. For slow body speeds, second-order terms $(u/w)^2$ are negligible, and we find

$$u = w \cdot \Delta\alpha. \quad (2)$$

This reduced-order model indicates that flight speed has a simple linear dependence on the paddling angle.

To experimentally validate this control law, we analyze the wing and body motions for the 16 sequences of forward flight. For each movie, we measure the full kinematics [16] and then extract the paddling angle, the mean speed of the wings, and the mean forward speed of the body. In Fig. 4(c), we plot the ratio of the body to wing speed versus the paddling angle. The prediction of the minimal model (dashed line) captures the observed linear relationship, and playing idealized paddling wing motions in the computational simulation (solid line) also yields a trend in agreement with the measurements. Collectively, these models and observations show how wing paddling is modulated to produce drag-based thrust in this flight mode.

Thus, though drag is commonly thought of as a hindrance, our discovery adds to the growing appreciation of its importance in aiding insect flight [14–18,21]. In particular this linear relation for forward speed [Eq. (2)] allows the insect to use simple flight speed control [22] and wing actuation [17] strategies. Moreover, calculations show that lift experiences only a weak, second-order decrease of $\Delta L/L \approx -(\Delta\alpha)^2$, which amounts to only 7% even for extreme paddling with $\Delta\alpha = 15°$. Thus paddling largely maintains the lift needed to keep aloft while recruiting drag for thrust.

Though we have highlighted pure paddling, more generally thrust is produced by both lift and drag which are associated with stroke-plane tilting and wing pitching, respectively. Indeed, qualitative observations of forward-flying insects in all 140 video sequences indicate that both modes are prevalent and used for both accelerating and steady flight. The fly's use of both strategies, in their pure forms and in combination, may reflect the near equivalence of the lift and drag coefficients at attack angles typical of insect flight [20]. Because this is a general feature of wings operating at intermediate Reynolds numbers [23], drag-based propulsion may be common among many flying insects.

An additional, and rather surprising, prediction of the reduced-order model is that flight speed does not depend on the fluid medium. In particular, the fluid density and drag coefficient do not appear in Eq. (2). However, this model assumes constant wing and body speeds within each stroke. In reality, unsteady body motions within a wing
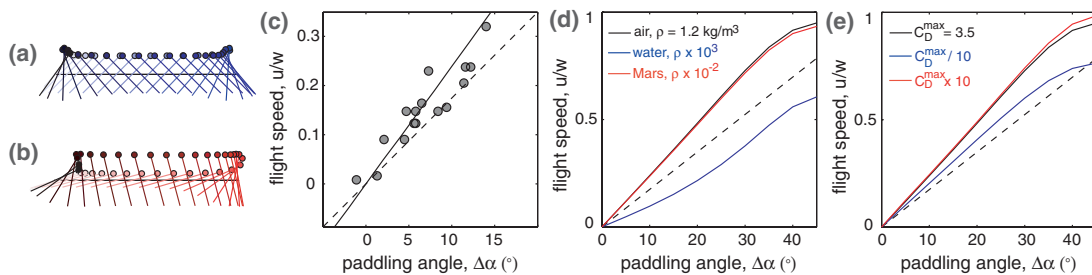

FIG. 4 (color). Paddling drives forward flight. (a) Hovering: each wing has equal attack angles for forward and backward sweeps. (b) Paddling: shifting the pitch downward by the paddling angle $\Delta\alpha$ (here, 30°) alters angle of attack. (c) Flight speed normalized by wing speed, u/w, correlates with $\Delta\alpha$. A minimal aerodynamic model [Eq. (2), dashed line] and simulation (solid line) account for the trend in the data (circles). Simulations show that the flight speed relation is insensitive to changes in the density of the fluid (d) and the drag coefficient (e).

beat can significantly modify the instantaneous wing air speed and thus the fluid forces generated. To determine whether these unsteady dynamics influence the flight speed control law, we again simulate paddling strokes [Figs. 4(a) and 4(b)], but vary the scale of the propulsive forces by changing the fluid density and drag coefficient. Figure 4(d) summarizes the dependence of flight speed on $\Delta\alpha$ for different density fluids. Paddling in air (black curve) and in lower density fluids such as the Martian atmosphere (red) give rise to similar flight speeds. Paddling in water (blue), which is a thousand times denser than air, leads to a slightly slower speed. Thus, while a given paddler may need to alter vertical force production in order to achieve level flight in different media, the horizontal speed law is relatively invariant to changes in fluid density. Similarly, increasing or decreasing the drag coefficient by a factor of 10 leads to only modest changes in this law [Fig. 4(e)].

This insensitivity of locomotion to material properties stems from a common physical origin of driving and resisting forces [4,11]. For flight of the fruit fly, these forces are dominated by pressure or form drag on the wings. Doubling the density, for example, doubles both the propulsive and resistive forces, leaving the velocity at which force balance is achieved unchanged. Thus, paddling locomotion is as effective in air as in water.

The use of common locomotion mechanisms in different media suggests that swimmers and flyers share similar adaptations for generating movement [11]. Such similarities may also shed light on the very origin of flight in insects. One evolutionary theory contends that the aerodynamic function of flapping appendages emerged from their use in underwater ventilation or swimming [24,25]. However, the seemingly great differences between swimming and flying have previously been viewed as evidence against this theory [26,27]. Instead, we interpret the use of common strategies as offering physical plausibility to the swimming-to-flying scenario. In particular, adaptations for swimming could have been co-opted for use in flight, and swimming would provide a context to evolve flapping appendages without the demands of weight support and stability. The plausibility of this transition is also supported by observations of insects that use wings for both swimming and flying [28,29] as well as by insects that row their wings while skimming on the surface of water [25].

[1] M. J. Lighthill, *Mathematical Biofluiddynamics* (SIAM, Philadelphia, 1975).

[2] S. Childress, *Mechanics of Swimming and Flying* (Cambridge University Press, Cambridge, 1981).

[3] T. Weis-Fogh, J. Exp. Biol. **59**, 169 (1973).

[4] S. Vogel, *Life in Moving Fluids* (Princeton University Press, Princeton, 1994).

[5] G. K. Taylor, R. L. Nudds, and A. L. R. Thomas, Nature (London) **425**, 707 (2003).

[6] S. Vogel, J. Exp. Biol. **44**, 567 (1966).

[7] S. Vogel, J. Exp. Biol. **46**, 383 (1967).

[8] R. Dudley and C. P. Ellington, J. Exp. Biol. **148**, 19 (1990).

[9] R. Dudley and C. P. Ellington, J. Exp. Biol. **148**, 53 (1990).

[10] A. P. Willmott and C. P. Ellington, J. Exp. Biol. **200**, 2705 (1997).

[11] M. W. Denny, *Air and Water: The Biology and Physics of Life's Media* (Princeton University Press, Princeton, 1993).

[12] F. E. Fish, American Zoologist **36**, 628 (1996).

[13] J. A. Walker and M. W. Westneat, Integr. Comp. Biol. **42**, 1032 (2002).

[14] Z. J. Wang, Phys. Rev. Lett. **85**, 2216 (2000).

[15] Z. J. Wang, J. Exp. Biol. **207**, 4147 (2004).

[16] L. Ristroph, G. J. Berman, A. J. Bergou, Z. J. Wang, and I. Cohen, J. Exp. Biol. **212**, 1324 (2009).

[17] A. J. Bergou, L. Ristroph, J. Guckenheimer, I. Cohen, and Z. J. Wang, Phys. Rev. Lett. **104**, 148101 (2010).

[18] L. Ristroph, A. J. Bergou, G. Ristroph, K. Coumes, G. J. Berman, J. Guckenheimer, Z. J. Wang, and I. Cohen, Proc. Natl. Acad. Sci. U.S.A. **107**, 4820 (2010).

[19] R. W. Blake, Symposia of the Zoological Society of London **48**, 29 (1981).

[20] M. H. Dickinson, F.-O. Lehmann, and S. P. Sane, Science **284**, 1954 (1999).

[21] T. L. Hedrick, B. Cheng, and X. Deng, Science **324**, 252 (2009).

[22] S. N. Fry, N. Rohrseitz, A. D. Straw, and M. H. Dickinson, J. Exp. Biol. **212**, 1120 (2009).

[23] S. P. Sane, J. Exp. Biol. **206**, 4191 (2003).

[24] V. B. Wigglesworth, Nature (London) **246**, 127 (1973).

[25] J. H. Marden and M. G. Kramer, Science **266**, 427 (1994).

[26] R. Dudley, *The Biomechanics of Insect Flight: Form, Function, Evolution* (Princeton University Press, Princeton, 2000).

[27] R. Dudley, G. Byrnes, S. P. Yanoviak, B. Borrell, R. M. Brown, and J. A. McGuire, Annu. Rev. Ecol. Evol. Syst. **38**, 179 (2007).

[28] H. Lubbock, Trans. Linn. Soc. Lond. **24**, 135 (1863).

[29] R. Matheson and C. R. Crosby, Annals of the Entomological Society of America **5**, 65 (1912).